A NEW 1:200,000-SCALE GEOLOGIC MAP OF TOOTING CRATER, MARS. Peter J. Mouginis-Mark, Hawai'i Institute of Geophysics and Planetology, Univ. Hawai'i, Honolulu, HI 96822, U.S.A. (pmm@hawaii.edu).

Introduction: Since the earliest days of the Viking Orbiter missions, the analysis of the lobate deposits surrounding many Martian impact craters has suggested the presence of water or ice within the top kilometer or more of the crust at the time of crater formation [1-3]. The terms "rampart crater" [4] and "single-layered", "double-layered", and "multi-layered ejecta craters" [5] have been used to describe these craters. Details of ejecta emplacement process may provide understanding of the rheology of the flows and the flow process [6, 7], as well as provide information on the possible interactions of target volatiles with impact melt generated during the event [8]. By virtue of its excellent degree of preservation and extensive coverage by high resolution images, Tooting crater, ~27.2 km in diameter, provides an outstanding opportunity to explore these relationships. Geologic mapping of Tooting crater (23°10'N, -152°10'E) has therefore been conducted at a scale of 1:200,000 using Thermal Emission Imaging System (THEMIS) visible (VIS) images (18 m/pixel) augmented by extensive use of data from the Context Imager (CTX) and High Resolution Imaging Science Experiment (HiRISE) scenes, with a ground sample distance of 6 m/pixel and 25 cm/pixel respectively (Fig. 1).

Mapped Units: Tooting crater formed within unit *Aa3*, interpreted by [9] as Late Amazonian lava flows. Previous studies [10 and 11] have identified numerous attributes of the crater cavity, including two distinct segments of a central peak (units *cph* and *cpm*), pitted material (*pm*) on the crater floor, numerous terrace block (*wb*) and flows on the interior walls, and impact melt on the rim crest. The mapping described here has revealed four discrete ejecta layers (el_1 to el_4) surrounding the crater (Fig. 1). The emplacement process was complex, with up to four different facies within each ejecta layer. The *smooth facies* is interpreted to indicate uniform flow with no relative velocity gradient within the layer. The *hummocky facies* is interpreted to characterize areas where ejecta flow overrode pre-existing topography, most likely created by earlier components of the ejecta due to the bland morphology of the surrounding target material. The *radial facies* is found down-range of discrete topographic obstacles such as large, partially buried secondary craters. The *crenulated facies* is predominately found close to the perimeter of the flow where the ejecta layer had continued to flow after the distal rampart (unit *dr*) had formed, causing a general disruption to the layer surface. 1,702 secondary craters >100 m dia. have been identified, as well as 315 buried secondary craters. The maximum range of the blocks that produced identifiable secondary craters is ~500 km (~36.0 crater radii) from the NE rim crest. In contrast, secondaries are only identifiable to ~215 km (15.8 radii) to the southeast and 225 km (16.5 radii) to the west. Crater clusters that comprise many tens of near circular craters a few tens of meters in diameter are seen to be aligned in linear chains radial to the crater center. In places crater clusters cross unit boundaries between el_1 and el_2, and in some places (such as to the NW) cross onto the pre-impact surface (unit Aa_3). Crater clusters can also be found that extend onto the distal ramparts.

Inferred Sequence of Events During Crater Formation: Four discrete episodes of ejecta emplacement can be identified, but these events may have been almost concurrent and probably took place only tens of seconds apart. Partially buried secondary craters located within ejecta layers el_1 and el_2 reveal that the outermost ejecta that were deposited by surface flow arrived at their maximum range after the ballistic component. Evidence for dewatering of the exterior rim materials (unit *erm*) after the ejecta came to rest, with the formation of lobate flows, has been documented for the southern rim as another late-stage event [10, 11]. The origin and time of formation of the crater clusters remains enigmatic; they appear to be late-stage features, except that on the western margin the craters appear to have been over-ridden by the distal ramparts associated with layer el_1.

It is not possible to directly correlate formation events within the crater cavity and the ejecta layers, but clearly both the interior and exterior units were formed almost at the same time. Inside the cavity, pitted material and smooth floor material were not deformed either by the uplift of the central peak or the collapse of the terrace blocks to produce the wall blocks on the floor. Smooth wall material formed late in the evolution of the crater because this material wraps around many of the wall blocks; at HiRISE resolution this smooth material can be seen to comprise flows that are interpreted to be remobilized by water leaking from the wall rocks [10, 11]. Where the smooth wall material extends onto the crater floor, it overlies the pitted material. Flows also exist within the rim units; HiRISE images show materials interpreted to be impact melt deposits flowing around previously formed terrace blocks [11].

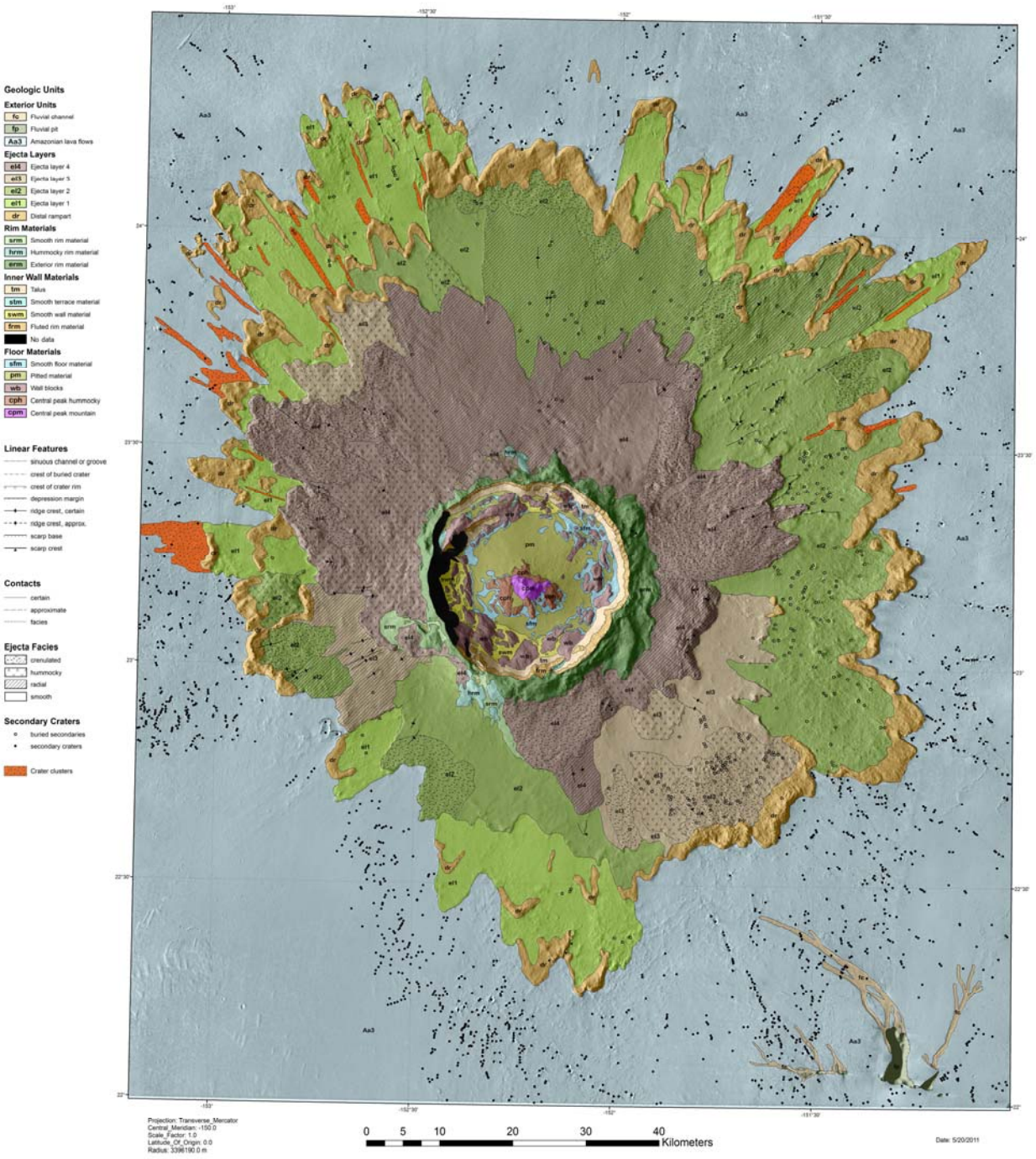

Figure 1: Formal geologic map of Tooting crater

References: [1] Carr, M. H. et al. (1977) *JGR* 82, 4055 - 4065. [2] Gault, D. E. & Greeley, R. (1978) *Icarus* 34, 486 – 495. [3] Mouginis-Mark, P. J. (1979) *JGR* 84, 8011 - 8022. [4] Mouginis-Mark, P. J. (1978) *Nature* 272, 691 - 694. [5] Barlow N. G. et al. (2000) *JGR* 105, 26,733 – 26,738. [6] Woronow, A. (1981) *Icarus* 45, 320 – 330. [7] Baloga, S.M. et al. (2005) *JGR* 110, E10001, doi:10.1029/2004JE002338. [8] Kieffer, S.W. & Simonds, C. H. (1980) *Rev. Geophys. Space Phys*. 18, 143 – 181. [9] Scott D. H. & Tanaka, K. L. (1986) *U.S. Geol. Survey Misc. Invest. Map* I-1082-A. [10] Mouginis-Mark, P. J. & Garbeil, H. (2007) *MAPS* 42, 1615 – 1625. [11] Morris, A. R. et al. (2010) *Icarus* 209, 369 – 389.